African Journal of Biological Sciences

Journal homepage: http://www.afjbs.com

Research Paper   Open Access

Impact of Alcoholic Environment on Hydrolysis of Phosphatidylcholine

Ikram S. Hussein[1], Thaer M. M. Al-Rammahi[2]*

[1,2]Department of Chemistry, College of Science, University of Kerbala, Karbala, Iraq.
*Corresponding Author's Email: thaer.alramahi@uokerbala.edu.iq

ABSTRACT

Phosphatidylcholine is a very important type of phospholipids in nature, and it has significant roles in the production of industrial materials in several sectors, including pharmaceutical, agricultural, and cosmetics, in addition to the food industry. This study has focused on the hydrolysis of phosphatidylcholine (PC) in different solvents; water and ethanol in acidic environments to find the effect of alcoholic environment on the hydrolysis process of this phospholipid. In this work, the hydrolysis reaction of PC has been investigated in the presence of hydrochloric acid (HCl) and ethanol (CH_3CH_2OH). The experiments were carried out in inert environment (in presence of N_2 as inert gas) using the Schlenk line technique to avoid the oxidative stresses. The data of ultraviolet/visible (UV. /Vis.) and infrared (IR) spectra were analysed using Origin 2019 software. Furthermore, all products were isolated and characterised using UV/Vis., FTIR, NMR spectrophotometers.The results showed that the hydrolysis of PC in both solvents undergoes the same mechanism of the reaction. The study has shown that there is clearly impacted on the products of the hydrolysis of phosphatidylcholine when using ethanol as a solvent.

Keywords: Phospholipids, Phosphatidylcholine, Lipolysis, Hydrolysis

1. Introduction

Phospholipids (PLs) are significant components in the living system, which play essential roles in the vital chemistry of various living organisms. In nature, there are thousands of phospholipids, which are broadly classified into sphingomyelin and glycerophospholipids such as phosphatidylserine (PS), phosphatidylcholine (PC), phosphatidylethanolamine (PE), phosphatidylinositol (PI) and phosphatidylglycerol (PG) [1-4]. The structure of PLs is based on a glycerol skeleton connecting a hydrophobic tail composed of two long-chain fatty acids linked to the positions sn-1, sn-2, and a hydrophilic head as phosphate group on the sn-3 position. In general, PC and PE are abundant phospholipids that are produced by biosynthetic enzymes, primarily in the endoplasmic reticulum [5].

Phospholipases are a complex group of enzymes, that play crucial roles in nature to hydrolysis of phospholipids into two freefatty acids and glycerophosphate compounds.Depending on the site of hydrolysis, phospholipases are classified as A1, A2, C, and D [6].Various studies were focused on understanding the pathways of lipolysis of PLs to finding the relationship between enzymatically modified PLs and pathogenic bacteria like Escherichia coli, Yersinia spp., Helicobacter pylori, Neisseria spp., and so forth [7-13]. Further efforts were performed at the laboratory to study and characterize the products of thehydrolysis of PLs in absence of phospholipases by using both acidic and alkaline environments [14-20]. Recent studies have considered the approachhydrolysis of PLs with respect to sustainability and process efficiency in presence of alcohol [21-23].

The present work aims to describe the hydrolysis mechanism of phosphatidylcholine at acidic media and investigate the effect of the alcoholic environment on the hydrolysis of this phospholipid hence suggesting the mechanism of the nucleophilic substitution reaction of fatty acids of phosphatidylcholine by the ethyl alcohol group.

2. Materials and Methods

Materials

Phosphatidylcholine (α-L-Lecithin, 98%) was obtained from Chemfish Tokyo Co., Ltd, hydrochloric acid (ACS reagent, 37%), ethanol absolute, and dimethyl sulfoxide-d^6 (DMSO-d^6, 99.8% for NMR spectroscopy) were provided by Sigma-Aldrich.

Methods

All experiments were performed at inert environment (in presence of N_2 as inert gas) using the Schlenk line technique.

The produced compounds were characterizedby using Shimadzu UV-1800 spectrophotometer and Shimadzu (FTIR-8400S) spectrophotometer at Department of Chemistry, College of Science University of Kerbala, Karbala, Iraq.

Bruker Avance III 400MHz NMR spectrometer was used to analyse the ^{1}H NMR, ^{13}C NMR and ^{31}P NMR for all characterized compounds. These NMR measurements were performed at the University of New South Wales (UNSW), Sydney, Australia.

The FTIR and UV/Vis. spectroscopy data for hydrolysis reaction of PC were analysed using Origin 2019 software provided by Origin Lab cooperation, Northampton, Massachusetts, USA.

Hydrolysis of Phosphatidylcholine in Hydrochloric Acid

Phosphatidylcholine (0.4 g) was added into a strongly acidic medium (50 ml, 2 N HCl). The mixture was stirred for 168h at 120 ˚C to complete thehydrolysis of PC.The progress of hydrolysis of PC was observed using thin layer chromatography (TLC), ultraviolet-visible (UV-Vis), and Fourier-transform infrared (FTIR) techniques at different times by withdrawing (1 ml) from the mixture of the reaction.

The colour of the mixture was light brown and gradually converts into dark brown with the appearance of the black fat layer on the surface of the mixture in the first hour of the reaction and increased further until the first twenty-four hours of the reaction. In addition, the white oily substance was produced after 44 to 55 h. At the end of the reaction, all produced substances were isolatedusing the appropriate separation methods.The final oily product was collected, purified, and characterized by NMR, FTIR, and UV-Vis. spectroscopy.

Hydrolysis of Phosphatidylcholine in Ethanol

This experiment was carried out under the same conditions as the above hydrolysis experiment.

A 0.4 g of PC was added into50 ml of absolute ethanol at strongly acidic environment pK_a= 1.2. The mixture was stirred for 150 h at 85°C. The reaction was also monitored by TLC, UV-Vis. and FTIR to compare with the results at different periods. All produced substances were isolated after 150 h using the appropriate separation methods. The black powder and brown fatty products wereisolated, purified, and characterized by NMR, FTIR, and UV-Vis. spectroscopy.
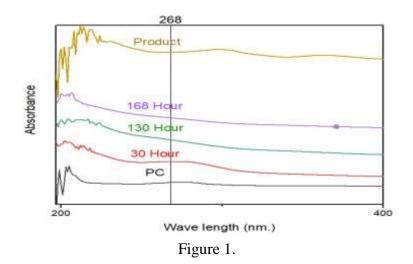
3. Results and Discussion

Monitoring of Hydrolysis of Phosphatidylcholine in Hydrochloric Acid

All experiments of PC hydrolysis in presence of HCl were generally observed using UV-Vis. and FTIR.

The UV-Vis. spectrum for PC before starting the hydrolysis shows a clear peak at λ_{max} =214 nm attributed to the n-π* transition of C=O for the ester. After 1h for the hydrolysis, it was noted that two peaks at λ_{max} =200 nm, and 212nm refer to the n-π* transition of C=O for free fatty acid and the ester of PC respectively. Constantly of the reaction time, the peak at 214 nm disappeared and only the peak at 200 nm was obtained, indicating the dissociation of the two groups of free fatty acids from the PC.The changes in the electronic absorption spectra of PC are shown in Table 1 and Fig. 1.

Table 1. The wavelengths and energies changes of PC during the hydrolysis in presence of HCl.

Time (h)	λ_{max}(nm)	Transition	Energy (Kcal/mole)
0	214	n-π* (C=O, ester)	133.6
1	212	n-π* (C=O, ester)	134.87
	200	n-π* (C=O, fatty acid)	142.96
5	210	n-π* (C=O, ester)	136.15
	198	n-π* (C=O, fatty acid)	144.4
10	210	n-π* (C=O, ester)	136.15
	200	n-π* (C=O, fatty acid)	142.96
30	214	n-π* (C=O, ester)	133.6
	202	n-π* (C=O, fatty acid)	141.54
45	210	n-π* (C=O, ester)	136.15
	199	n-π* (C=O, fatty acid)	143.68
75	198	n-π* (C=O, fatty acid)	144.4
130	200	n-π* (C=O, fatty acid)	142.96
145	200	n-π* (C=O, fatty acid)	142.96
168	201	n-π* (C=O, fatty acid)	142.25

Figure 1.

UV-Vis.Spectra for the hydrolysis of PC in presence of HCl. Black curve is a spectrum of PC before the reaction. Red curve is a spectrum of PC at 30 h of the reaction. Green curve is a spectrum of PC at 130 h of the reaction. Purple curve is a spectrum of PC at 168 h of the reaction. Brownish yellow curve is a spectrum of the final product (Glycerol-3-phosphate).
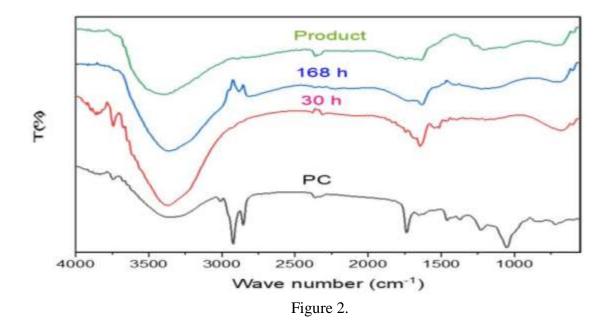
The observations of FTIR spectra exhibited thatat zero time of reaction, the strong peak at 1735 cm^{-1}attributed to stretching of C=O ester group in addition to further medium peaks at 2854cm^{-1} and 2924cm^{-1} refer to stretching of C-H for alkane and alkene respectively that peaks can be attributed to the two associated fatty acids for PC, and another medium peak at 3363cm^{-1} refers to stretching of N-H for aliphatic aminefor choline.

After one hour of reaction, the new strong peak at 3430 cm^{-1}for OH group appeared which indicates to dissociative of one fatty acid from PC and form aliphatic alcohol. By continuation of the reaction, it can be noted that the peak at 1735 cm^{-1} gradually disappeared. At the end of the hydrolysis reaction, the FTIR spectra showed increase in the intensity of OHfor aliphatic alcohols as a result of substituting of two hydroxyl groups instead of two fatty acids on the backbone of glycerol to form the glycerol-3-phosphate as a final product of hydrolysis reaction for the PC, see table 2 and figure 2.

Table 2. Characteristic of FTIR peaks of PC functional groups during the hydrolysis in presence of HCl.

Time (h)	Position of peak (cm^{-1})	Intensity	Group	Notes
0	3363	m	N-H (v)	Choline[24]
	3009-2924	m	C-H (v)	Alkene of FA[25]
	2854	m	C-H (v)	Alkane of FA[25, 26]
	1735	s	C=O (v)	Ester[25, 26]
	1647	w	C=C (v)	Alkene of FA[25]
	1230	m	C-N (v)	Choline[24]
	597	w	P-O(v)	Phosphate [27]
1	3430	s	O-H (v)	Alcohol [27]
	1739	s	C=O (v)	Ester[25, 26]
	1651	w	C=C (v)	Alkene of FA at sn-2[25]
	1211	m	C-N (v)	Choline[24]
	605	w	P-O (v)	Phosphate[27]
5	3380	br, s	O-H (v)	Alcohol[27]
	1643	w	C=C (v)	Alkene of FA at sn-2[25]

	1226	m	C-N (ν)	Choline[24]
	602	w	P-O (ν)	Phosphate [27]
10	3364	br, s	O-H (ν)	Alcohol[27]
	1709	m	C=O (ν)	Carboxylic of free FA[25]
	1640	w	C=C (ν)	Alkene of free FA[25]
	1230	m	C-N (ν)	Choline[24]
	598	w	P-O (ν)	Phosphate[27]
30	3364	br, s	O-H (ν)	Alcohol[27]
	1196	w	C-N (ν)	Choline[24]
	602	w	P-O (ν)	Phosphate[27]
45	3379	br, s	O-H (ν)	Alcohol[27]
	1709	m	C=O (ν)	Carboxylic of free FA[25]
	1640	w	C=C (ν)	Alkene of free FA[25]
	1227	w	C-N (ν)	Choline[24]
	602	w	P-O (ν)	Phosphate[27]
75	3364	br, s	O-H (ν)	Alcohol[27]
	1712	w	C=O (ν)	Carboxylic of free FA[25]
	1647	w	C=C (ν)	Alkene of free FA[25]
	1223	w	C-N (ν)	Choline[24]
	598	w	P-O (ν)	Phosphate[27]
130	3364	br, s	O-H (ν)	Alcohol[27]
	1651	w	C=C (ν)	Alkene of free FA[25]
	1210	w	C-N (ν)	Choline[24]
	602	w	P-O (ν)	Phosphate[27]
145	3368	br, s	O-H (ν)	Alcohol[27]
	602	w	P-O (ν)	Phosphate[27]
168	3360	br, s	O-H (ν)	Alcohol[27]
	602	w	P-O (ν)	Phosphate[27]

Figure 2.

FTIR Spectra for the hydrolysis of PC in presence of HCl. Black curve is a spectrum of PC before the reaction. Red curve is a spectrum of PC at 30 h of the reaction. Blue curve is a

spectrum of PC at 168 h of the reaction. Green curve is a spectrum of the final product (Glycerol-3-phosphate).

At the end of the hydrolysis reaction of PC, the main three final products which include the glycerol-3-phosphate, free fatty acid, and choline chloride were isolated and characterized using NMR and FTIR spectroscopy.

The ^{1}HNMR spectrum of glycerol-3-phosphate in DMSO-d[6]: δ 1.23-1.16 (doublet-doublet, 2 H, sn-1 CH_2), δ 2.73 (singlet, 1 H, sn-2 CH), δ 3.31(singlet, 1 H, sn-1 OH), δ 4.02-4.04 (doublet-doublet, 2 H, sn-3 CH_2), and δ 5.32 (singlet, 1 H, sn-2 OH), as shown in figure 3.

The ^{13}C NMR spectrum of glycerol-3-phosphate in DMSO-d[6]: δ 63.2 (1 C, sn-1 CH_2), δ 72.7 (1 C, sn-2 CH), and δ 73.9 (1 C, sn-3 CH_2), as shown in figure 4.

The ^{31}P NMR spectrum of glycerol-3-phosphate in DMSO-d[6]: δ – 1.48 (singlet, 1 P, sn-3 PO_4^{-2}), as shown in figure 5.

The FTIR spectrum of glycerol-3-phosphate showed the strong broad peak at 3371 cm^{-1}attributed to stretching of sn-1 OH and sn-2 OH groups, medium peak at 2897 cm^{-1}attributed to stretching of C-H alkane at sn-1, sn-2, sn-3 positions, and the weak peak at 598 cm^{-1} refer to P-O of PO_4^{-2} group, as shown in figure 6.
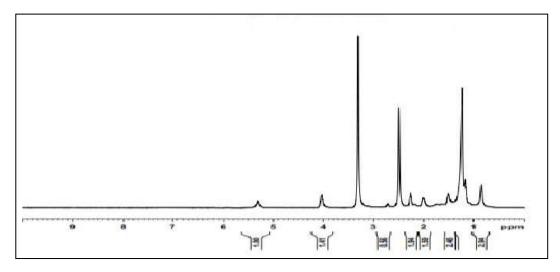

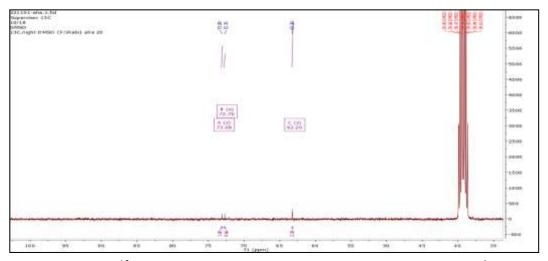Figure 3.^{1}H NMR spectrum of glycerol-3-phosphate in DMSO-d[6].

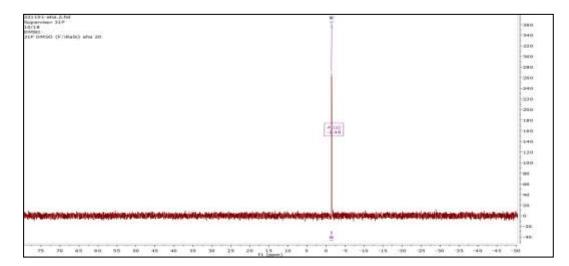Figure 4. ^{13}C NMR spectrum of glycerol-3-phosphate in DMSO-d[6].

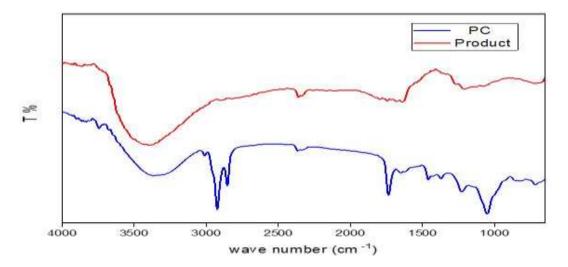Figure 5. ^{31}P NMR spectrum of glycerol-3-phosphate in DMSO-d^6.

Figure 6. distinguish between the FTIR spectra of PC and glycerol-3-phosphate. Blue curve is a spectrum of PC, and the red curve is a spectrum of glecerol-3-phosphate as final product for the hydrolysis reaction of PC.

The ^{1}H NMR spectrum of free fatty acid in DMSO-d^6: δ1.07 (triplet, 3 H, CH$_3$), δ 2.32 – 2.45 (multiplet, 20 H, CH$_2$), δ 3.11 – 3.72 (multiplet, 8 H, CH$_2$), δ 5.22 - 5.63 (doublet – doublet, 4 H, CH$_2$), and δ 8.52 (singlet, 1 H, OH carboxylic acid), as shown in figure 7.

The ^{13}C NMR spectrum of free fatty acid in DMSO-d^6 showed 18 peaks of C: δ 14.42, δ 14.59, δ 28.18, δ 30.08, δ 37.98, δ 53.58, δ 53.62, δ 53.65, δ 55.55, δ 57.89, δ 62.91, δ 63.49, δ 71.03, δ 72.34, δ 72.96, δ 73.06, δ 73.22, and δ 75.70, as shown in figure 8.

The FTIR spectrum of free fatty acid showed medium broad peak at 3429 cm^{-1} indicate to stretching O-H group of fatty acid, other peaks at 3009 cm^{-1}, 2924 cm^{-1}, and 2854 cm^{-1} attributed to stretching of C-H alkane, and strong peak at 1709 cm^{-1} refer to stretching of C=O fatty acid, as shown in figure 9.
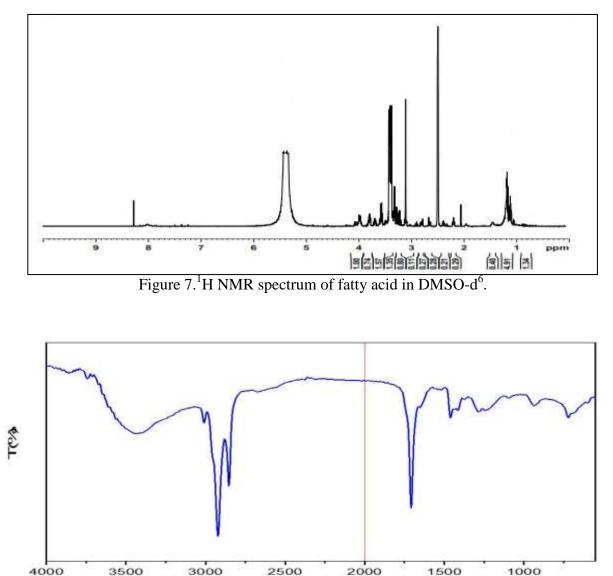

Figure 7. ^{1}H NMR spectrum of fatty acid in DMSO-d^{6}.

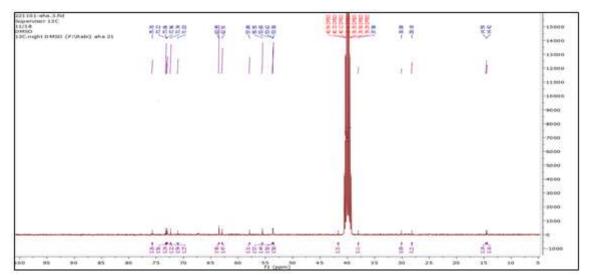Figure 8. ^{13}C NMR spectrum of fatty acid in DMSO-d^{6}.

Figure 9. FTIR spectrum for the fatty acid as the byproduct for the hydrolysis reaction of PC.

The ^{1}H NMR spectrum of choline chloride in DMSO-d^6: δ 3.34 (singlet, 9H, CH$_3$), δ 3.65 (doublet-doublet, 2H, CH$_2$), δ 3.86 (doublet-doublet, 2H, CH$_2$), and δ 5.17 (singlet, 1H, OH), as shown in figure 10.

The ^{13}C NMR spectrum of choline chloride in DMSO-d^6: δ 22.44 (1 C, CH$_2$OH), δ 29.19 (1 C, CH$_3$), δ 29.5 (2 C, CH$_3$), and 31.37 (1 C, CH$_2$), as shown in figure 11.

The FTIR spectrum of choline chloride exhibited a medium broad peak at 3472 cm^{-1} attributed to stretching O-H bond, strong peak at 2940 cm^{-1} refer to stretching of C-H alkane, and weak peak at 1259 cm^{-1} attributed to stretching C-N aliphatic amine, as shown in figure 12.
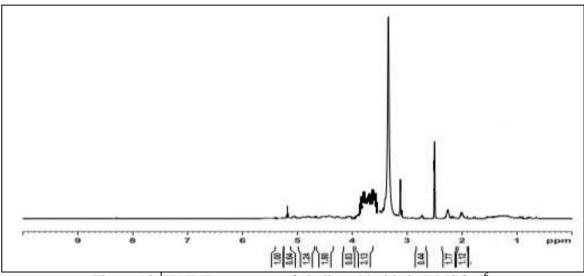

Figure 10. ^{1}H NMR spectrum of choline chloride in DMSO-d^6.

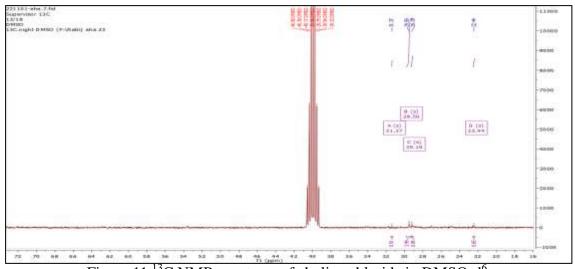Figure 11. ^{13}C NMR spectrum of choline chloride in DMSO-d^6.

Depending on the above results, it likely seems that the mechanism of the hydrolysis of PC includes main three steps. The first step is the protonation of carbonyl groups at sn-1 and sn-2, and phosphate at sn-3positions followed by water attack as a nucleophilic agent. At the second step of mechanism, the proton will transfer into the oxygen of the ester bond followed by dissociative of the free fatty acid groups from sn-1 and sn-2 positions. The next step includes forming of an intra-hydrogen bond between the hydrogen of sn-2 OH and the oxygen of phosphatefollowed by protonation of the oxygen for the choline which leads to dissociative as choline chloride, as shown in figure 13.
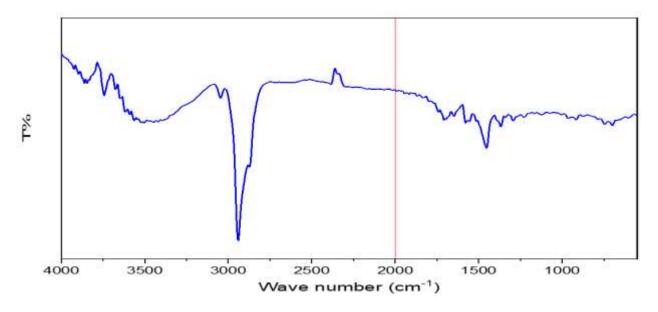

Figure 12.FTIR spectrum of choline chlorideas byproduct of the hydrolysis of PC.
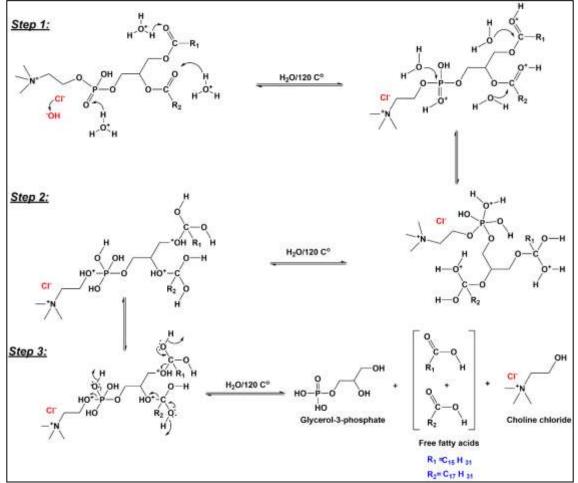
Figure 13. The proposed mechanism for the hydrolysis reaction of PC in the presence of HCl.

Monitoring of Hydrolysis of Phosphatidylcholine in Ethanol

The reaction of the hydrolysis of PC in the presence of ethanol in an acidic environment was also observed by using UV/Vis. and FTIR spectroscopy.

The UV/Vis spectra of PC during the hydrolysis reaction are slightly impacted due to using ethanol as a solvent, as shown in table 3. In addition, it can be noted that the ethanol plays an important role throughout the hydrolysis reaction of PC. At zero time of the reaction, the UV/Vis. spectrum of PC showed a peak at $\lambda = 279$ nm, which is attributed to n-π* transition of carbonyl for the PC ester group. After one hour of the PC hydrolysis reaction, the spectrum exhibited two peaks at $\lambda = 281$ nm refer to n-π* transition of C=O for the PC ester group and another peak at $\lambda = 212$ nm refer to produce new ethyl ester with the fatty acid residue at PC. The monitoring of the change in UV/Vis. spectra during the hydrolysis reaction of PC in the presence of ethanol provided good evidence about the dissociative of fatty acid as ethyl fatty ester instead of leaving the PC as free fatty acid. At the end of the reaction, the absorbance at the $\lambda_{max} \approx 212$ nm increased and the absorbance at the $\lambda \approx 280$ nm decreased, which could be attributed to form high concentrations of ethyl fatty ester during the hydrolysis of PC in presence of ethanol, Figure 14.

Table 3. The wavelengths and energies changes of PC during the hydrolysis in presence of ethanol.

Time (h)	λ_{max}(nm)	Transition	Energy (Kcal/mole)
0	279	n-π* (C=O, PC ester)	102.48

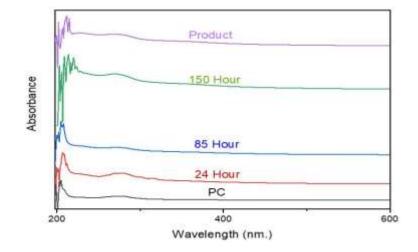| 1 | 281 | n-π* (C=O, PC ester) | 101.75 |
	212	n-π* (C=O, ethyl fatty ester)	134.87
5	283	n-π* (C=O, PC ester)	101.03
	215	n-π* (C=O, ethyl fatty ester)	132.98
24	275	n-π* (C=O, PC ester)	103.97
	212	n-π* (C=O, ethyl fatty ester)	134.87
45	279	n-π* (C=O, PC ester)	102.48
	213	n-π* (C=O, ethyl fatty ester)	134.23
85	268	n-π* (C=O, PC ester)	106.68
	211	n-π* (C=O, ethyl fatty ester)	135.5
100	258	n-π* (C=O, PC ester)	110.82
	210	n-π* (C=O, ethyl fatty ester)	136.15
150	268	n-π* (C=O, PC ester)	106.68
	212	n-π* (C=O, ethyl fatty ester)	134.87

Figure 14. UV-Vis. Spectra for the hydrolysis of PC in presence of ethanol.

Black curve is a spectrum of PC before the reaction. Red curve is a spectrum of PC at 24 h of the reaction. Blue curve is a spectrum of PC at 85h of the reaction. Green curve is a spectrum of PC at 150 h of the reaction. Purple curve is a spectrum of PC of the final product (Ethyl fatty ester).

The monitoring of the FTIR spectra for the hydrolysis of PC in ethanol appeared a slight change in the principle peaks due to the production of the ethyl fatty acid that has the same active C=O ester group as the PC. However, the new strong broad peak at 3330 cm^{-1} appeared after one hour of the reaction, and this peak is attributed to stretching of the O-H bond for the glycerol-3-phosphate as a main product for the hydrolysis reaction of the PC, as shown in table 4 and figure 15.

Table 4. Characteristic of FTIR peaks of PC functional groups during the hydrolysis in presence of ethanol.

Time (h)	Position of peak (cm^{-1})	Intensity	Group	Notes
0	3290	br, w	N-H (v)	Choline [24]
	2978	m	C-H (v)	Alkene of FA [25]
	2890	m	C-H (v)	Alkane of FA [25, 26]

	1735	s	C=O (ν)	Ester [25, 26]
	1647	w	C=C (ν)	Alkene of FA [25]
	1260	m	C-N (ν)	Choline [24]
	601	w	P-O (ν)	Phosphate [27]
1	3330	s	O-H (ν)	Alcohol [27]
	1740	m	C=O (ν)	Ester [25, 26]
	1662	w	C=C (ν)	Alkene of FA at sn-2[25]
	1273	w	C-N (ν)	Choline [24]
	602	w	P-O (ν)	Phosphate [27]
5	3306	br, s	O-H (ν)	Alcohol [27]
	2974	m	C-H (ν)	Alkene of FA [25]
	2893	w	C-H (ν)	Alkane of FA [25, 26]
	1651	w	C=C (ν)	Alkene of FA at sn-2[25]
	1273	w	C-N (ν)	Choline [24]
	602	w	P-O (ν)	Phosphate [27]
24	3329	br, s	O-H (ν)	Alcohol [27]
	2974	s	C-H (ν)	Alkene of FA [25]
	1674	w	C=C (ν)	Alkene of FA at sn-2[25]
	1381	m	O-H (δ)	Alcohol [27]
	1273	w	C-N (ν)	Choline [24]
	601	w	P-O (ν)	Phosphate [27]
45	3340	br, s	O-H (ν)	Alcohol [27]
	2978-2928	m	C-H (ν)	Alkene of FA [25]
	1739	m	C=O (ν)	Ester of Ethyl FA ester[25]
	1651	w	C=C (ν)	Alkene of free FA [25]
	1381	m	O-H (δ)	Alcohol [27]
	1250	w	C-N (ν)	Choline [24]
	606	w	P-O (ν)	Phosphate [27]
85	3352	br, s	O-H (ν)	Alcohol [27]
	2987	m	C-H (ν)	Alkene of FA [25]
	2897	m	C-H (ν)	Alkane of FA [25, 26]
	1739	m	C=O (ν)	Ester of Ethyl FA ester [25]
	1678	w	C=C (ν)	Alkene of free FA [25]
	1381	m	O-H (δ)	Alcohol [27]
	1223	w	C-N (ν)	Choline [24]
	601	w	P-O (ν)	Phosphate [27]
100	3321	br, s	O-H (ν)	Alcohol [27]
	2979	m	C-H (ν)	Alkene of FA [25]
	2901	m	C-H (ν)	Alkane of FA [25, 26]
	1739	w	C=O (ν)	Ester of Ethyl FA ester [25]
	1675	w	C=C (ν)	Alkene of free FA [25]
	1377	m	O-H (δ)	Alcohol [27]
	1226	w	C-N (ν)	Choline [24]
	601	w	P-O (ν)	Phosphate [27]
150	3365	br, s	O-H (ν)	Alcohol [27]
	3009	m	C-H (ν)	Alkene of FA [25]
	2875	m	C-H (ν)	Alkane of FA [25, 26]
	1739	w	C=O (ν)	Ester of Ethyl FA ester [25]
	1645	w	C=C (ν)	Alkene of free FA [25]
	1376	m	O-H (δ)	Alcohol [27]

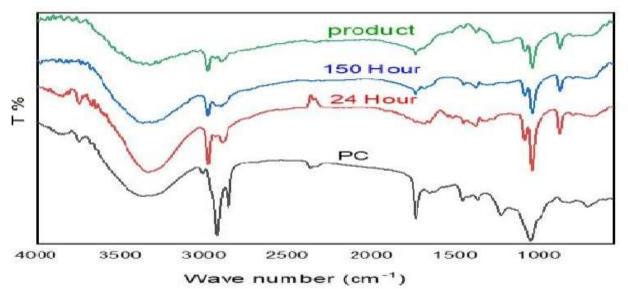| | | 1223 | w | C-N (v) | Choline [24] |
| | | 602 | w | P-O (v) | Phosphate [27] |

Figure 15. FTIR Spectra for the hydrolysis of PC in presence of ethanol. Black curve is a spectrum of PC before the reaction. Red curve is a spectrum of PC at 24 h of the reaction. Blue curve is a spectrum of PC at 150 h of the reaction. Green curve is a spectrum of the final product (Ethyl fatty ester).

At the end of the hydrolysis reaction of PC in ethanol, all final products were separated and characterized using NMR and FTIR spectroscopy.

The measurements of the main product of PC hydrolysis (glycerol-3-phosphate) provided the same results for ^{1}H NMR, ^{13}C NMR, ^{31}P NMR, and FTIR, see figures (3-6).

In addition, the ^{1}H NMR, ^{13}C NMR, and FTIR of the choline chloride were the same that elaborate above, see figures (10-12).

The ^{1}H NMR spectrum of ethyl fatty ester in DMSO-d[6]: δ 0.89 (triplet, 3 H, CH_3), δ 1.08 (triplet, 3 H, CH_3), δ 2.1 (singlet, 2 H, CH_2), δ 3.32 – 3.8 (multiplet, 10 H, CH_2), and δ 4.8 - 5.1 (doublet – doublet, 20 H, CH_2), as shown in figure 16.

The ^{13}C NMR spectrum of free fatty acid in DMSO-d[6] showed 20 peaks of C: δ 14.33, δ 14.7, δ 28.3, δ 31.1, δ 37.98, δ 41.44, δ 41.66, δ 53.56, δ 53.60, δ 53.64, δ 55.73, δ 58.88, δ 63.01, δ 63.51, δ 71.11, δ 72.64, δ 72.77, δ 73.09, δ 73.32, and δ 75.8, as shown in figure 17.

The FTIR spectrum of free fatty acid showed strong peaks at 2926 cm^{-1}, and 2854 cm^{-1} attributed to stretching of C-H alkane, the strong peak at 1737 cm^{-1} refer to stretching of C=O fatty ester, medium peak at 1620 cm^{-1} attributed to the bending C-H alkane, and other medium peaks at 1462 cm^{-1}, 1456 cm^{-1}, and 1371 cm^{-1} indicate to the bending C-H for methyl group, as shown in figure 18.
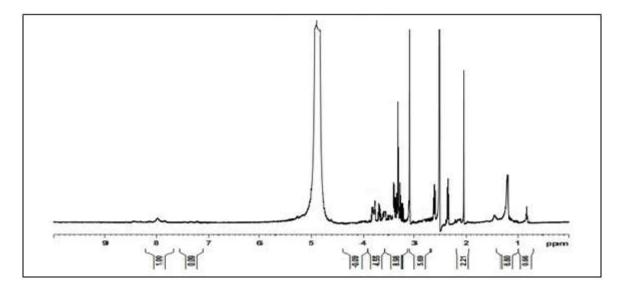
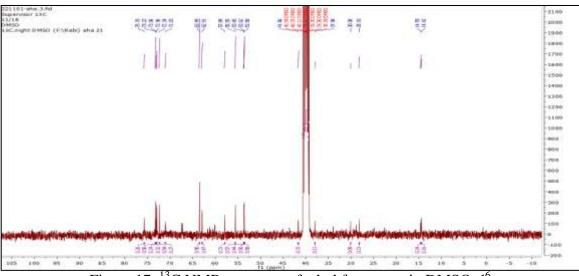Figure 16. ^{1}H NMR spectrum of ethyl fatty ester in DMSO-d^6.

Figure 17. ^{13}C NMR spectrum of ethyl fatty ester in DMSO-d^6.
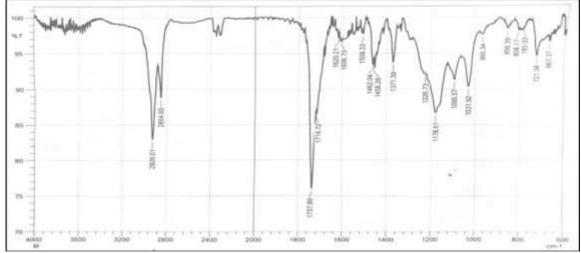

Figure 18. FTIR spectrum for the ethyl fatty ester as the byproduct for the hydrolysis reaction of PC in ethanol.

The mechanism of the hydrolysis reaction of PC in presence of ethanol at pKa =1.2 can be proposed as presented in figure 19.
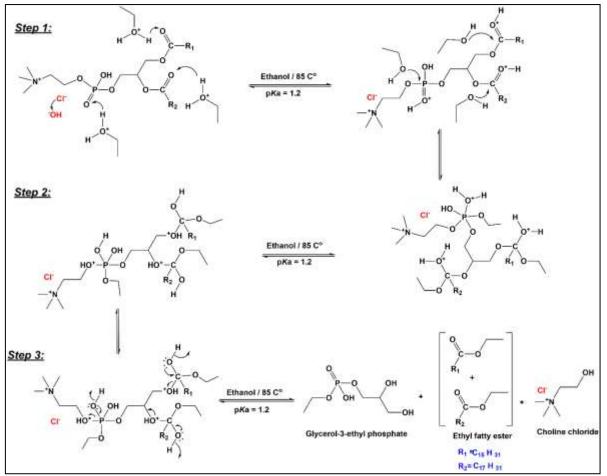

Figure 19. The proposed mechanism for the hydrolysis reaction of PC in the presence of ethanol at pKa= 1.2.

4. Conclusions

During the monitoring of the hydrolysis reactions of phosphatidylcholine in different environments (water and ethanol), it likely seems that the mechanisms of bothreactions are the same. However, the final products of these reactions were slightly different due to differences in the substituted groups. Consequently, the hydrolysis of PC in water resulted the glycerol-3-phosphate as a main product in addition to free fatty acids and choline chloride as byproducts. The ethyl fatty ester was formed as the byproduct of the hydrolysis of PC in ethanol.

Despite the similarity in mechanisms of the hydrolysis in both solvents, the differences in byproducts may provide us with a good vision to predict the impact of the solvent on this process. Due to the various applications of phosphatidylcholine, understanding of the effect of the alcoholic environmentcan help pharmaceutical, cosmetic, and food factories to design appropriate experiments to reduce the impact of these byproducts on the main product efficiency and yield.

5. References

1. A.H. Ali, X. Zou, S.M. Abed, S.A. Korma, Q. Jin, X. Wang, Natural phospholipids: Occurrence, biosynthesis, separation, identification, and beneficial health aspects, Critical Reviews in Food Science and Nutrition 59 (2019) 253-275.

2. A. Avalli, G. Contarini, Determination of phospholipids in dairy products by SPE/HPLC/ELSD, Journal of chromatography. A 1071 (2005) 185-190.

3. A.A. Christy, P.K. Egeberg, Quantitative determination of saturated and unsaturated fatty acids in edible oils by infrared spectroscopy and chemometrics, Chemometrics and Intelligent Laboratory Systems 82 (2006) 130-136.

4. A. G Hassabo, Saturated Fatty Acids Derivatives as Assistants Materials for Textile Processes, Journal of Textile Science & Fashion Technology 1 (2018).

5. D.C. Wilton, CHAPTER 11 - Phospholipases, in: D.E. Vance, J.E. Vance (Eds.), Biochemistry of Lipids, Lipoproteins and Membranes (Fifth Edition), Elsevier, San Diego, 2008, pp. 305-329.

6. D.E. Williams, K.B. Grant, Metal-Assisted Hydrolysis Reactions Involving Lipids: A Review, Front Chem 7 (2019) 14.

7. E.M. White, A.R. Holland, G. MacDonald, Infrared studies reveal unique vibrations associated with the PGK-ATP-3-PG ternary complex, Biochemistry 47 (2008) 84-91.

8. F. Bleffert, J. Granzin, M. Caliskan, S.N. Schott-Verdugo, M. Siebers, B. Thiele, L. Rahme, S. Felgner, P. Dörmann, H. Gohlke, R. Batra-Safferling, K.E. Jaeger, F. Kovacic, Structural, mechanistic, and physiological insights into phospholipase A-mediated membrane phospholipid degradation in Pseudomonas aeruginosa, eLife 11 (2022).

9. F. Mancin, L.J. Prins, P. Pengo, L. Pasquato, P. Tecilla, P. Scrimin, Hydrolytic Metallo-Nanozymes: From Micelles and Vesicles to Gold Nanoparticles, Molecules, 2016.

10. G. Contarini, M. Povolo, Phospholipids in milk fat: composition, biological and technological significance, and analytical strategies, International journal of molecular sciences 14 (2013) 2808-2831.

11. G. Gimenez, K.G. Magalhães, M.L. Belaunzarán, C.V. Poncini, E.M. Lammel, S.M. Gonzalez Cappa, P.T. Bozza, E.L. Isola, Lipids from attenuated and virulent Babesia bovis strains induce differential TLR2-mediated macrophage activation, Molecular immunology 47 (2010) 747-755.

12. H. Sato, Y. Taketomi, M. Murakami, Metabolic regulation by secreted phospholipase A(2), Inflammation and regeneration 36 (2016) 7.

13. H. Yang, R. Woscholski, A Novel High-Throughput Assay Reveals That the Temperature Induced Increases in Transphosphatidylation of Phospholipase D Are Dependent on the Alcohol Acceptor Concentration, Biomolecules 12 (2022).

14. J. Kaur, Phospholipases in Bacterial Virulence and Pathogenesis, Advances in Biotechnology & Microbiology 10 (2018).

15. J.E. Burke, E.A. Dennis, Phospholipase A2 structure/function, mechanism, and signaling1, Journal of Lipid Research 50 (2009) S237-S242.

16. K. Rathnakumar, J. Ortega-Anaya, R. Jimenez-Flores, S.I. Martínez-Monteagudo, Understanding the switchable solvent extraction of phospholipids from dairy byproducts, Food and Bioproducts Processing 126 (2021) 175-183.

17. K. Mulia, E. Krisanti, F. Terahadi, S. Putri, Selected Natural Deep Eutectic Solvents for the Extraction of α-Mangostin from Mangosteen (Garcinia mangostana L.) Pericarp, International Journal of Technology 6 (2015).

18. L.A. Colin, Y. Jaillais, Phospholipids across scales: lipid patterns and plant development, Current Opinion in Plant Biology 53 (2020) 1-9.

19. L. Yu, F.-z. Li, J.-y. Wu, J.-q. Xie, S. Li, Development of the aza-crown ether metal complexes as artificial hydrolase, Journal of Inorganic Biochemistry 154 (2016) 89-102.

20. M.J. Ormsby, E. Grahame, R. Burchmore, R.L. Davies, Comparative bioinformatic and proteomic approaches to evaluate the outer membrane proteome of the fish pathogen Yersinia ruckeri, Journal of Proteomics 199 (2019) 135-147.

21. Ms. Rashmi Dubey, Dr. Ujwala Bendale, & Ms. Mayura Pawar. (2022). Provisions for Protection against Child Prostitution: A Study. Journal of Legal Subjects(JLS) ISSN 2815-097X, 2(06), 1–8. https://doi.org/10.55529/jls.26.1.8

22. Mohammed Jibril. (2021). Effect of Firms Attributes on Non-Performing Loans of Listed Deposit Money Banks in Nigeria. Journal of Corporate Finance Management and Banking System (JCFMBS) ISSN : 2799-1059, 1(01), 26–41. https://doi.org/10.55529/jcfmbs11.26.41

23. Manisha Sharma, & Dr. Anita Rana. (2022). A Comparative Study of Committee's Reports on Corporate Governance in India. Journal of Corporate Finance Management and Banking System (JCFMBS) ISSN : 2799-1059, 2(03), 36–51. https://doi.org/10.55529/jcfmbs.23.36.51

24. N.E. Wezynfeld, T. Frączyk, W. Bal, Metal assisted peptide bond hydrolysis: Chemistry, biotechnology and toxicological implications, Coordination Chemistry Reviews 327-328 (2016) 166-187.

25. O. Quehenberger, S. Dahlberg-Wright, J. Jiang, A.M. Armando, E.A. Dennis, Quantitative determination of esterified eicosanoids and related oxygenated metabolites after base hydrolysis, J Lipid Res 59 (2018) 2436-2445.

26. Orkhan Sultanov. (2022). Comparative Analysis of the Level of Liberality of the Banking System Across Countries. Journal of Corporate Finance Management and Banking System (JCFMBS) ISSN : 2799-1059, 2(04), 36–39. https://doi.org/10.55529/jcfmbs.24.36.39

27. Olalere Victor Dotun, & Anthony Kolade Adesugba. (2022). The Impact of Agency Banking on Financial Performance of Listed Deposit Money Banks in Nigeria. Journal of Corporate Finance Management and Banking System (JCFMBS) ISSN : 2799-1059, 2(05), 14–24. https://doi.org/10.55529/jcfmbs25.14.24

28. S.J. AL-Shaeli, A.M. Ethaeb, H.A. Gharban. Determine the glucose regulatory role of decaffeinated Green Tea extract in reduces the metastasis and cell viability of MCF7 cell line. In AIP Conference Proceedings, 2394 (2022), 1-8.

29. S Ramesh. (2022). A Study of Law Regarding Life Insurance Business in India. Journal of Legal Subjects(JLS) ISSN 2815-097X, 2(05), 10–14. https://doi.org/10.55529/jls.25.10.14

30. Sumathy, D. M. ., & Das, A. S. . (2022). A Study on Mutual Fund Investors' Awareness. Journal of Corporate Finance Management and Banking System (JCFMBS) ISSN: 2799-1059, 2(02), 22–28. https://doi.org/10.55529/jcfmbs.22.22.28

31. Subhasmita Rana. (2022). Public Education Expenditure and Economic Growth: an Econometric Analysis. Journal of Corporate Finance Management and Banking System (JCFMBS) ISSN: 2799-1059, 2(04), 40–45. https://doi.org/10.55529/jcfmbs.24.40.45

32. T.M. Al-Rammahi, R.A. Henderson, Exploring the acid-catalyzed substitution mechanism of [Fe4S4Cl4](2-), Dalton Trans 45 (2016) 307-314.

33. T. Namani, R.J. Ruf, I. Arsano, R. Hu, C. Wesdemiotis, N. Sahai, Novel Chimeric Amino Acid-Fatty Alcohol Ester Amphiphiles Self-Assemble into Stable Primitive Membranes in Diverse Geological Settings, Astrobiology 23 (2023) 327-343.

34. Veronica Muda, Oscar Agyemang Opoku, Jerry Anim, & Isaac Opoku-Dadzie. (2022). The Effect of Job Satisfaction on Staff Retention and Attrition at GCB Bank PLC in Upper East Region of Ghana. Journal of Corporate Finance Management and Banking System (JCFMBS) ISSN: 2799-1059, 2(04), 25–35. https://doi.org/10.55529/jcfmbs.24.25.35

35. X. Wang, C.J. Swing, T. Feng, S. Xia, J. Yu, X. Zhang, Effects of environmental pH and ionic strength on the physical stability of cinnamaldehyde-loaded liposomes, Journal of Dispersion Science and Technology 41 (2020) 1568-1575.

36. Y. Hayakawa, R. Nakayama, N. Namiki, M. Imai, Promising Immobilization of Industrial-Class Phospholipase A1 to Attain High-Yield Phospholipids Hydrolysis and Repeated Use with Optimal Water Content in Water-in-Oil Microemulsion Phase, Applied Sciences, 2021.

37. Yasar Imam, & Prof. Anwar Khurshid Khan. (2021). Role of Microfinance in Entrepreneurial Development of Women in India. Journal of Corporate Finance Management and Banking System (JCFMBS) ISSN: 2799-1059, 1(02), 1–10. https://doi.org/10.55529/jcfmbs.12.1.10